Preprints.org

Article

Not peer-reviewed version

Application of κ-Carrageenan for One-Pot Synthesis of Hybrids of Curcumin Natural with Iron and Copper: Stability Analysis and Application in Papilloscopy

Danielle Tapia Bueno , Amanda Fonseca Leitzke , Juliana Porciúncula da silva , Daisa Hakbart Bonemann , Gabrielly Quartieri Sejanes , Bruno Nunes da Rosa , Tais Poletti , Guilherme Kurz Maron , Bruno Vasconcellos Lopes , Matheus de Paula Goularte , Darci Alberto Gatto , André Luiz Missio , Neftali Lenin Villareal Carreno , Claudio Martin Pereira de Pereira *

Posted Date: 10 October 2024

doi: 10.20944/preprints202410.0766.v1

Keywords: Curcumin; hybrid materials; stability in solution; thermal stability; papilloscopy

Preprints.org is a free multidiscipline platform providing preprint service that is dedicated to making early versions of research outputs permanently available and citable. Preprints posted at Preprints.org appear in Web of Science, Crossref, Google Scholar, Scilit, Europe PMC.

Copyright: This is an open access article distributed under the Creative Commons Attribution License which permits unrestricted use, distribution, and reproduction in any medium, provided the original work is properly cited.

Preprints.org (www.preprints.org) | NOT PEER-REVIEWED | Posted: 10 October 2024 doi:10.20944/preprints202410.0766.v1

Disclaimer/Publisher's Note: The statements, opinions, and data contained in all publications are solely those of the individual author(s) and contributor(s) and not of MDPI and/or the editor(s). MDPI and/or the editor(s) disclaim responsibility for any injury to people or property resulting from any ideas, methods, instructions, or products referred to in the content.

Article

Application of *K*-Carrageenan for One-Pot Synthesis of Hybrids of Curcumin Natural with Iron and Copper: Stability Analysis and Application in Papilloscopy

Danielle Tapia Bueno [1,2], Amanda Fonseca Leitzke [1,3], Juliana Porciúncula da Silva [1], Daisa Hakbart Bonemann [1,2], Gabrielly Quartieri Sejanes [1], Bruno Nunes da Rosa [1,2], Taís Poletti [1,2], Guilherme Kurz Maron [2], Bruno Vasconcellos Lopes [3], Matheus de Paula Goularte [2,4], Darci Alberto Gatto [4], André Luiz Missio [2], Néftali Lenin Villarreal Carreno [2] and Claudio Martin Pereira de Pereira [1,2,3,*]

[1] Center of Chemical, Pharmaceutical and Food Sciences, Innovation and Solutions in Chemistry Laboratory, Federal University of Pelotas, Eliseu Maciel St., s/n, Pelotas, RS 96900-010, Brazil.
[2] Postgraduate Program in Materials Science and Engineering, Technology Development Center, Federal University of Pelotas, 96010-000 Pelotas, Rio Grande do Sul, Brazil.
[3] Postgraduate Program in Biotechnology, Federal University of Pelotas, 96000-010 Pelotas, Rio Grande do Sul, Brazil.
[4] Center for Engineering, Wood Physical and Mechanical Properties Laboratory, Wood Science Research Group, Federal University of Pelotas, 012 Dona Mariana Street - Center, Pelotas, RS 96010-450, Brazil.
* Correspondence: claudiochemistry@gmail.com

Abstract: In this study, hybrid materials were synthesized incorporating curcumin, Cu^{2+} or Fe^{3+}, and *Kappa*-carrageenan as a reducing agent to improve its stability, considering that curcumin has low thermal and solution stability, which limits its applications. Colorimetric analysis showed color changes in the hybrids, ultraviolet-visible spectroscopy revealed band shifts in the hybrids, and infrared analysis indicated shifts in wavenumbers, suggesting changes in the vibrational state of curcumin after bonding with metal ions. These techniques confirmed the formation of the hybrid materials. Thermogravimetric and chromatographic analyses demonstrated greater thermal and solution stability for the hybrids compared to curcumin. Additionally, the hybrid composites effectively developed natural and sebaceous latent fingerprints with good clarity and contrast on glass surfaces. Both composites performed similarly to commercial gold powder. When applied to surfaces representative of forensic scenarios, the composites were versatile, revealing sufficient fingerprint details for human identification on both porous and non-porous surfaces. Scanning electron microscopy images showed greater clarity in sebaceous and natural fingerprints developed with the Fe composite compared to the Cu composite, due to minimal interaction of Fe with the glass surface.

Keywords: curcumin; hybrid materials; stability in solution; thermal stability; papilloscopy

1. Introduction

Papilloscopy refers to the science dedicated to studying fingerprints, which vary between individuals and even on the same person. This uniqueness has made fingerprints a reliable method of human identification for over a century [1]. In forensic sciences, fingerprints analysis is based on Locard's exchange principle, which establishes that every contact between two objects results in a transfer of traces between them. Consequently, the act of touching a surface transfers material from the ridges of the fingers onto a surface [2]. In criminal investigations, fingerprints are considered physical evidence, as they not only capture the pattern ridges but can also retain exogenous compounds such as drugs, explosives, and chemicals [3]. Latent fingerprints (LFPs) found at crime scenes are invisible to the naked eye and require specific methods to be visualized, which include optical (ultraviolet laser), chemical (cyanoacrylate fuming), and physical (powder dusting and

© 2024 by the author(s). Distributed under a Creative Commons CC BY license.

Preprints.org (www.preprints.org) | NOT PEER-REVIEWED | Posted: 10 October 2024 doi:10.20944/preprints202410.0766.v1

deposition [4,5]. One of the oldest and still widely used techniques by forensic experts is the powder technique, especially when LFPs are deposited on smooth surfaces such as glass, metal, and plastic. The technique is simple, involving the application of powder with a specific brush onto the surface where the LFP is found, making the ridges patterns and their minutiae visible to the naked eye [6]. An ideal compound for developing fingerprint should provide high contrast, good adhesion properties, and desirable selectivity [1]. In this context, the search for a selective, high-contrast, low-cost, and reliable powder for developing LFPs has been relentless. Most LFP powders available use hazardous chemicals in their synthesis, and continuous use can cause side effects. Therefore, the use of natural products as a raw material source for the development of new LFP developers' is of great interest, as their use may result in a final product with little to no toxicity [7].

Based on this, curcumin, a natural dye extracted from the rhizomes of Curcuma longa, has emerged as a promising candidate [8]. Its structure comprises a β-diketone fraction, methoxy groups, phenolic hydroxyls, doubly conjugated bonds, and keto-enol tautomerism [9]. Studies reports that the properties found in Turmeric are mainly attributed to curcumin, making the isolated compound of great interest [10]. Interesting properties of isolated curcumin have been reported, which includes high antimicrobial activity [11], antibacterial properties [12], antioxidant features [13], among others. However, isolated curcumin exhibits rapid photodegradation when exposed to light [14] and air [15], which limits its stability and effectiveness. Furthermore, the curcumin molecule is not stable in solution due to the β-diketone fraction of curcumin, which is a hydrolytic center. This hydrolytic center is involved in the elimination of the hydroxyl radical and in redox reactions, leading to the formation of degradation products, that is, minor phenolics [14], such as ferulic acid, vanillic acid and vanillin [16]. To overcome these limitations, hybrid materials can be designed from various components in order to achieve original properties in a single material [17]. The β-diketone groups enable curcumin to chelate metal ions, leading to the formation of hybrid materials, which comprises by a combination of two or more phases, whether organic or inorganic with unique properties [18]. However, the properties of a hybrid material are not merely a sum of the individual contributions of its constituents, depending on the chemical nature of the organic and inorganic compounds. Due to their complexity, they can be classified in different categories. Among all, the most usual classification is performed according to the type of interaction or nature of the chemical bonds between the organic and inorganic components. As mentioned earlier, curcumin contains a fraction that acts as a strong chelating agent, and thus, hybrid materials synthesized from curcumin belong to class II, which consists of materials formed through covalent or ionic bonds [19]. For the synthesis of a hybrid material containing curcumin and a metal as organic and inorganic phases, respectively, a third phase with metal-reducing properties is needed. In this scenario, the use *Kappa*-carrageenan (κ-car) as a reducer agent has attracted interest [20] κ-car is a polysaccharide extracted from red macroalgae, featuring non-toxic, low-cost, edible, biodegradable and biocompatible properties [21]. The negatively charged surface of κ-car enables easy interaction with positively charged metal ions through electrostatic attraction. Moreover, the presence of hydroxyl (OH) groups facilitates the reduction of these metals [22].

According to what has been reported, in this work, we continue our efforts to develop derivatives of organic compounds with application in papilloscopy [7,23–32]. Therefore, this study reports the development of a new hybrid material of curcumin and *Kappa*-carrageenan combined with two low-cost copper and iron metals. The hybrid materials were evaluated for thermal stability and solution behavior. Finally, these hybrid composites were tested as potential LFO developers, offering a novel, low-toxicity alternative for fingerprint analysis.

2. Materials and Methods

The curcumin (diferuloylmethane, 65 % purity) and *Kappa*-carrageenan were purchased from Sigma-Aldrich (St. Louis, USA). Acetonitrile was purchased from Biograde (North Carolina, USA – HPLC ≥ 99.99%). Tetrahydrofuran (THF) was purchased from Honeywell (North Carolina, USA – HPLC ≥ 99.99%). Fingerprint powder developer Gold® was purchased from Sirchie® (Youngsville, USA). Other chemicals were of analytical grade from commercial sources.

Preprints.org (www.preprints.org) | NOT PEER-REVIEWED | Posted: 10 October 2024 doi:10.20944/preprints202410.0766.v1

Synthesis of the hybrid materials

The hybrid materials were synthesized following a one-pot methodology adapted from Li et al., (2021) [33]. Briefly, in a beaker, was added copper acetate monohydrate (Cu(CO2CH3)2 · H2O, Vetec-P.A) (0.1359 g, 0,0012 mmol) or iron (III) chloride hexahydrate (FeCl3 · 6H2O, Vetec-P.A) (0.1834 g, 0.0008 mmol) was added into curcumin (1 – Scheme 1) (0.5 g, 0.0014mmol) previously dissolved in a solution of ethanol (8 mL) and deionized water (4 mL). Then, *Kappa*-carrageenan (1 g, 0.0023 mmol) was added to the mixture in the beaker, which reacted for 30 minutes at room temperature. The mixture was rinsed with of deionized water (200 mL) and absolute ethanol (200 mL). Finally, the material was centrifuged (10 min, 4.000 rpm) to separate the solid-liquid phases. The solid fraction was dried in an oven at 60°C for 2 hours. The Scheme 1 presents the synthesis of new hybrid materials (2 – Scheme 1).

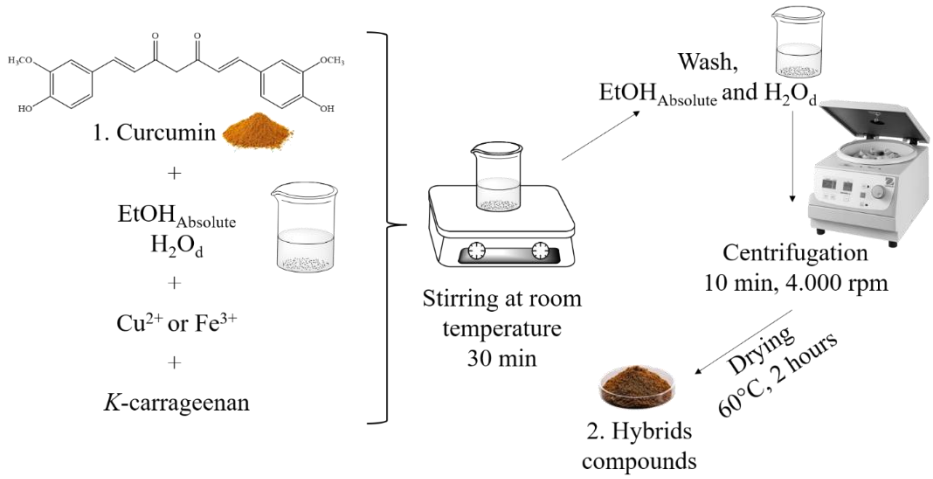

Scheme 1. Scheme of the synthesis of new hybrid materials.

Characterization

The Ultraviolet-Visible Spectroscopy (UV-Vis) of pure curcumin and both Fe and Cu hybrid materials was performed in a Bel LGS53 instrument, with the samples diluted in methanol solvent. The samples were also investigated by Fourier Transform Infrared Spectroscopy (FT-IR, Shimadzu SPIRIT instrument), using potassium bromide (KBr - [0.5%]). X-Ray Diffraction (XRD) patterns were recorded in the 2θ range from 10° to 60° in a Shimadzu XRD-6000 instrument. Thermogravimetric Analysis (TGA) was performed in Shimadzu DTG-60 instrument. The samples were evaluated in N2 atmosphere, from 30 to 800 °C and heating rate of 10 °C/min. To determine the color of the samples, *Kappa*-carrageenan, curcumin, copper acetate, iron chloride, copper hybrid and iron hybrid samples were analyzed in a CR-400 colorimeter (Konica Minolta), with an observation angle of 10 °, calibrated with porcelain, configured with D65 light. All analyses were performed in triplicate. The CIELab system (L*, a* and b*) was used to determine the colorimetric parameters. In this system, L* represents lightness (from 0 (black) to 100 (white)), a* corresponds to the green-red axis (negative values indicate shades of green, while positive values indicate shades of red), and b* corresponds to the axis blue-yellow (negative values indicate shades of blue, while positive values indicate shades of yellow). To identify the variation between colors, ΔE was used, according to the following Equation (1.0):

$$\Delta E = \{(\Delta L)^2 + (\Delta a)^2 + (\Delta b)^2\}1/2 \quad (1.0)$$

where ΔE is the variation of all colors; ΔL is the variation in lightness; Δa is the variation in the red-green coordinate; and Δb is the variation in the blue-yellow coordinate [33].

High-Performance Liquid Chromatography with UV-Vis Detector (HPLC-UV-Vis)

The chromatographic analyses were performed using a Thermo Scientific Ultimate 3000, Waltham model, USA, with a standard auto-injector and UV-Vis detector. The separation of analytes

Preprints.org (www.preprints.org) | NOT PEER-REVIEWED | Posted: 10 October 2024 doi:10.20944/preprints202410.0766.v1

was carried out on an C18 column (Ascentis, Bellevue, USA) with a particle size of 5 μM, a pore size of 90 Å, and 15 cm x 4.6 mm in size. For the determination of curcuminoids in the commercial curcumin sample, the adapted method [34], where the isocratic mode was used with a mobile phase of 0.001% phosphoric acid (in water) and acetonitrile (20:80, v/v). The analysis was performed at a temperature of 45 ^{0}C, with an injection volume of 20 μL, a flow rate of 0.8 mL/min, for 5 minutes. The detection wavelength was 425 nm, and the samples were diluted in acetonitrile.

For the determination of the solution stability of curcumin and the hybrid materials, the method employed was adapted from Kumar et al., (2021) [16]. The isocratic mode was used, and a mobile phase mixture was employed: acetonitrile, tetrahydrofuran, and 2% acetic acid (aqueous) (26.3:63.2:10.5 v/v). The analysis was carried out at room temperature for 7 minutes. The injection volume was 20 μL, the flow rate was 1 mL/min, detection was achieved at 254 nm, and the samples were dissolved in acetonitrile. The analysis was conducted by program time: time zero (immediately after sample dilution), after 2 hours and after 24 hours of aging (reference time zero).

Preparation of Hybrid Composites

An adapted methodology previously described by Modwi was used to prepare the Fe and Cu hybrid composites [25]. Briefly, copper or iron precursor, silver mica powder, carboxymethyl cellulose, and cellulose acetate were combined in the proportions of (20:15:15:50), respectively. The mixture was added to 200 mL of absolute ethyl alcohol the solution was sonicated in an ultrasonic bath for 30 minutes. The resulting solution was transferred to a container of a dispersing mill (PE-075), where 150 g of zirconia beads and 50 mL of ethyl alcohol were added. The composites were processed for 3 hours at a rotation speed of 18000 RPM. The final solution was centrifuged for 10 minutes at 4000 RPM. The supernatant was discarded, and the powder were dried in an oven at 100 °C for 4 hours.

Determination of the Concentration of Cu and Fe in Hybrids

For the determination of Cu and Fe elements, the hybrids were first digested through an acid digestion process in a digestion block (Tecnal, Piracicaba, Brazil), following the methodology described by Fioravante [36]. Thus, 0.25 g of the samples were weighed into a glass tube, and 5 mL of nitric acid was added. The mixture was heated in a digestion block for 2 hours at 100°C. Subsequently, 2 mL of hydrogen peroxide was added, and the solution was returned to the digestion block for another 2 hours at 100°C. After cooling, the content was transferred to polypropylene tubes and brought to a volume of 12 mL with deionized water.

The elements were quantified using a flame atomic absorption spectrometer (F AAS), model AAnalyst 200 (Perkin Elmer, Singapore), equipped with a hollow cathode lamp for each analyte to be determined (Lumina, Perkin Elmer) and a deuterium arc lamp as a background corrector. Additionally, acetylene (Linde, Barueri, SP, Brazil) was used as the fuel gas, and compressed air as the oxidant gas. The calibration curve was prepared from a 1000 mg L^{-1} standard containing the elements to be determined.

Papilloscopy

For fingerprint development, the powder technique was used with the aid of specific brushes (132LBW and CFB100, acquired from Sirchie®). The developed fingerprints were then photographed with a Canon EOS Rebel T6 18MP digital camera, with the close-up + 4 58-mm lens, distance of 9 cm, focus 5.6, and automatic ISO speed photo mode. For better visualization, three white led lamps were used to improve the brightness with a black background under the fingermarks. The fingermark images were processed in the Adobe Photoshop software. All the surfaces used for deposition and development of fingerprints were washed with water and neutral soap after being photographed. All the photos taken were deleted after the publication of this work. The method of Pacheco et al., (2021) [28] was used for the deposition of natural and sebaceous fingerprints. Natural fingerprints are those that donors deposit after 30 minutes of washing their hands. For sebaceous prints, donors were asked

Preprints.org (www.preprints.org) | NOT PEER-REVIEWED | Posted: 10 October 2024 doi:10.20944/preprints202410.0766.v1

to rub their thumbs on sebaceous parts of the face such as the forehead or nose. Natural and sebaceous fingerprints, a depletion series, and a comparison with standard gold powder adquired from Sirchie® were evaluated.

The evaluation of latent, natural, and sebaceous fingerprints from four donors, developed with Copper and Iron hybrid composites, was carried out according to the scale proposed by Sears et al., (2012) [37] (Table S1 – Supplementary information). This assessment was conducted by five independent analysts, all of whom hold Bachelor's degrees in Forensic Chemistry from the Federal University of Pelotas. To determine the final score, located to the left of the respective image in each corresponding figure, the most frequently assigned evaluation among the five analysts was chosen.

For SEM analysis, a Shimadzu SSX-550 Superscan was used. A glass slide was used as the substrate for the deposition of natural and sebaceous fingerprints, which were further developed with the Fe and Cu hybrid materials. The substrate was fixed with carbon tape, gold-coated, and analyzed at 15 kV. Secondary electron imaging was used along with the following analytical parameters: AccV of 15.0 kV and a 4.0 probe.

3. Results

The influence of metals on the color of hybrid materials was observed and the images are shown in Figure 1. It was observed that curcumin (Figure 1B) and *Kappa*-carrageenan (Figure 1C) exhibit saffron yellow and whitish colors, respectively. Additionally, after the addition of *Kappa*-carrageenan in curcumin (Figure 1E), only the hue was altered, while the overall color remained unchanged, which agrees with the L*, a*, and b* values, as indicated in Table S2 (Supplementary information). In the presence of metals (Figures 1 F and G), significant changes in the color of the materials were clearly noticed. As shown in Table 1, the a* and b* values for the copper hybrid material (a* 9.10 and b* 58.44) and the iron hybrid material (a* 2.41 and b* 11.98) decreased compared to the values obtained for the curcumin/*Kappa*-carrageenan mixture (a* 16.46 and b* 82.17), suggesting that the red and yellow components were reduced. Among the hybrid materials, the copper hybrid exhibited the highest red and yellow values, indicating that Cu 2+ has a more significant role in enhancing the color of curcumin/*Kappa*-carrageenan. Additionally, the L* values were reduced for the copper (L* 43.92) and iron (L* 14.33) hybrid materials, indicating that they exhibited a darker color compared to the curcumin/*Kappa*-carrageenan (L* 63.40), which is consistent with reports from the literature [33]. Additionally, when determining the concentration of Cu and Fe in the hybrid materials, values of 13.31 and 13.51 mg g-1, respectively, were obtained, thus confirming the presence of the metals in their respective hybrid materials.

Figure 1. A - Copper Acetate; B – curcumin; C - *Kappa*-carrageenan; D - iron chloride; E - curcumin/*kappa*-carrageenan; F - copper hybrid; G - iron hybrid.

Preprints.org (www.preprints.org) | NOT PEER-REVIEWED | Posted: 10 October 2024 doi:10.20944/preprints202410.0766.v1

Conform, Figure 2A show the UV–Vis spectrum of curcumin, Cu and Fe hybrid materials. The curcumin exhibited a maximum absorption at the wavelength of 425 nm and a weak absorption at 262 nm [38]. The samples containing Cu an Fe exhibited more intense absorption bands, with a shift of approximately 6 nm [39]. Furthermore, bands at 419 nm and 255 nm were clearly observed for the Cu hybrid material, while peaks at 428 nm and 257 nm are observed for the Fe hybrid material. The crystal structure of samples was further investigated through XRD and the results are presented in Figure 2B. The XRD pattern of curcumin exhibits its typical crystal structure with intense peaks, especially at angles below 30 degrees, similar to what has been reported in other similar studies [40]. For the *Kappa*-carrageenan samples an amorphous structure was observed, similar as reported by other authors [41]. The amorphous behavior remained predominant for the hybrid samples, where no peaks corresponding to the crystal planes could be identified. The FT-IR was used to identity the functional groups on the surface of the samples and the results are displayed in Figures 2C and D. The infrared spectra of curcumin show a typical band at 3461 cm-1 corresponding to the phenolic stretching (O-H). Thus, the aromatic stretching (C=C) and stretching vibrations (C=C) were observed at 1629 cm-1 and 1509 cm-1, respectively. The stretching vibrations (C=O) are observed at 1599 cm-1, the bending vibrations (C-H) and aromatic stretching (C-O) vibrations were noticed at 1427 cm-1 and 1280 cm-1, respectively. Finally, the stretching vibrations (C-O-C) are observed at 1025 cm-1 [42]. The FT-IR of the Fe and Cu hybrid materials exhibit similar bands as observed in the curcumin. Furthermore, the vibrations mode suffered shifts in their wavenumber indicating changes in the vibrational state of curcumin upon binding to the metal ions [43,44].

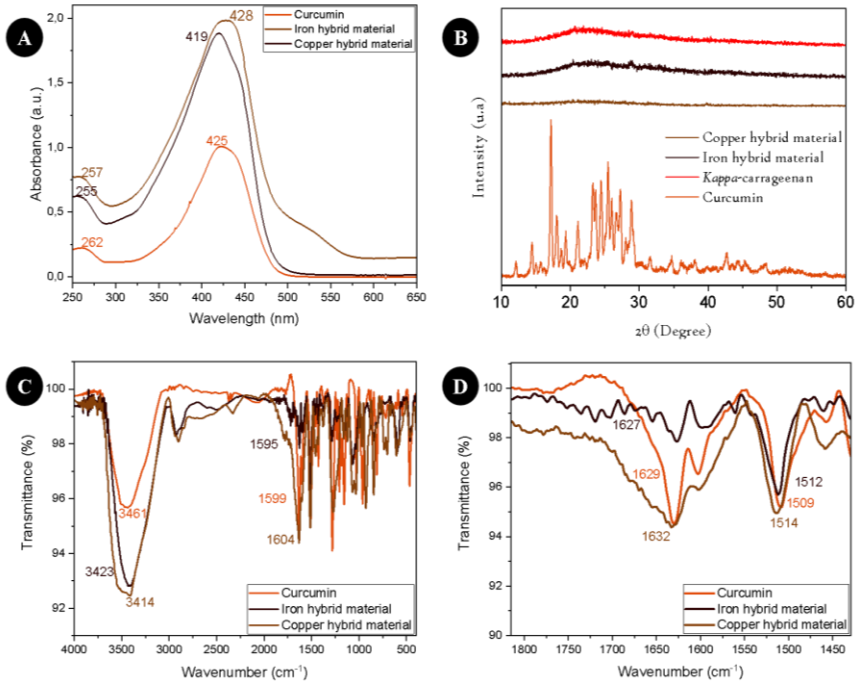

Figure 2. A) UV-Vis spectra; B) X-ray diffractogram; C) FT-IR spectra; D) zoomed FT-IR spectra.

TGA of the hybrid materials, curcumin, and *Kappa*-carrageenan were performed, and the results are shown in Figure 3. *Kappa*-carrageenan (Figure 3A) exhibited three stages of weight loss, which is consistent with previous reports [45]. The first thermal event occurred around 218 °C. The second and third thermal event occurred at approximately 531 °C and 747 °C, respectively. The decomposition of curcumin began around 333 °C, with total degradation occurring around 575 °C, reaching 45.43%, which is in accordance with literature reports. The TGA curve for Curcumin/*Kappa*-carrageenan (Figure 3B) showed three stages of mass losses of 12.43%, 14.29%, and 10.46% at temperatures of 207 °C, 342 °C, and 722 °C, respectively. Finally, two and three stages of mass loss were observed for the iron and copper hybrid materials, respectively. Both samples exhibited the

Preprints.org (www.preprints.org) | NOT PEER-REVIEWED | Posted: 10 October 2024 doi:10.20944/preprints202410.0766.v1

greatest mass loss in the first thermal event, 17.25% and 18.12%, at temperatures of 198 °C and 229 °C, respectively [33].

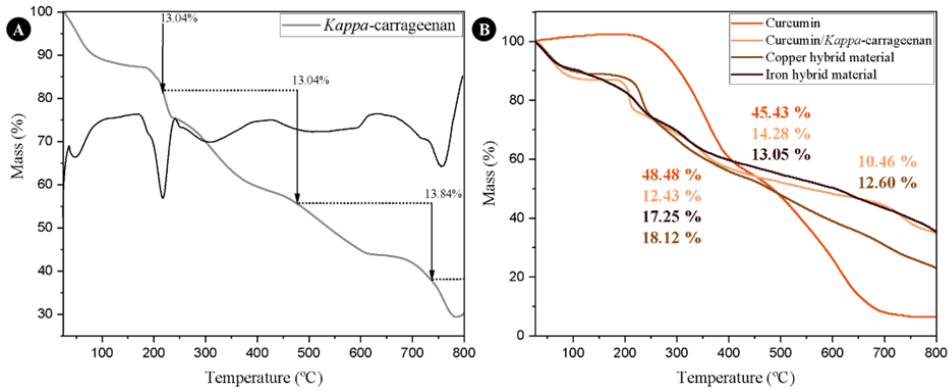

Figure 3. TGA curves of (A) *Kappa*-carrageenan, (B) Curcumin, Curcumin/*Kappa*-carrageenan and hybrids materials.

In the analysis of curcuminoids in a commercial sample of natural curcumin, three distinct peaks were observed, as shown in Figure S1 (Supplementary information). Peak 1 has a retention time of 2.957 minutes, Peak 2 has a retention time of 3.103 minutes, and Peak 3 has a retention time of 3.263 minutes. In the study of curcumin and hybrid material degradation, the samples were injected into the HPLC at different time intervals starting from the moment of dissolution. During this period, the samples were incubated in clear glass vials and left in an unprotected light area throughout the analysis period. Figure 4A shows the chromatograms of the curcumin solution at different time points, while Figure 4B presents the chromatogram of the curcumin solution after 24 hours, where the presence of more than one peak can be noted. In Figures 4C and 4D, the chromatograms of copper and iron hybrid materials, respectively. It can be observed that new peaks were not detected after 24 hours.

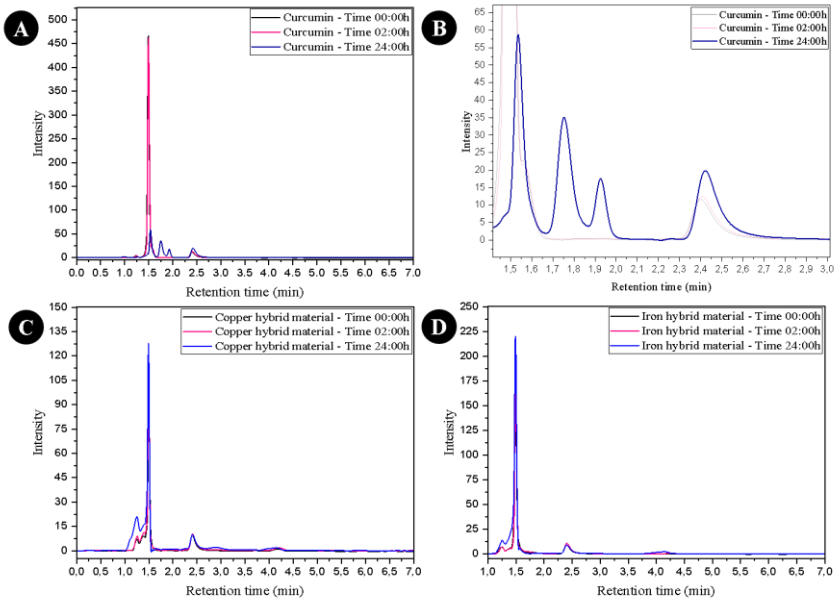

Figure 4. a) Chromatogram of the analyzed curcumin solution at different time intervals; b) Enlargement of the curcumin chromatogram at the 24:00h time point; c) Chromatogram of the analyzed copper hybrid material solution at different time intervals; d) Chromatogram of the analyzed iron hybrid material solution at different time intervals.

Preprints.org (www.preprints.org) | NOT PEER-REVIEWED | Posted: 10 October 2024 doi:10.20944/preprints202410.0766.v1

In the development of fingerprints using composites generated from hybrid materials, an initial study was conducted with a variety of donors. To convert the visual appearance of the fingerprints developed with powders into numerical values, and recognizing that the researchers of this study are not fingerprint identification experts, a scoring system was employed instead of relying solely on minutiae detection and counting. This scoring system has been in use for over 35 years. The fingerprint evaluation scheme is presented in Table S1 (Supplementary Information). Cu and Fe composites were then applied to develop fingerprints using the physical powdering method on a glass surface. Figures 5 and 6 show the natural and sebaceous fingerprints from four donors, along with their respective scores.

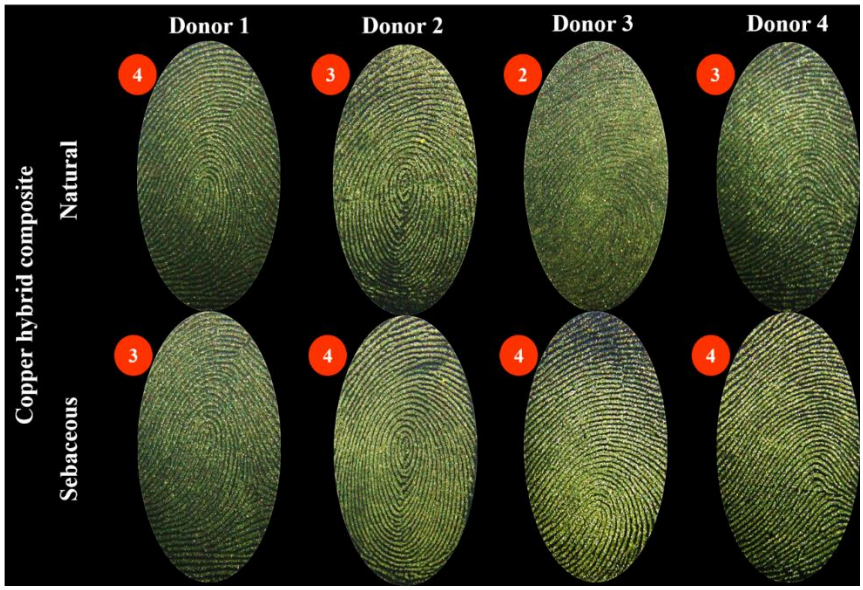

Figure 5. Natural and sebaceous fingerprints developed with the Cu hybrid composite and their respective scores.

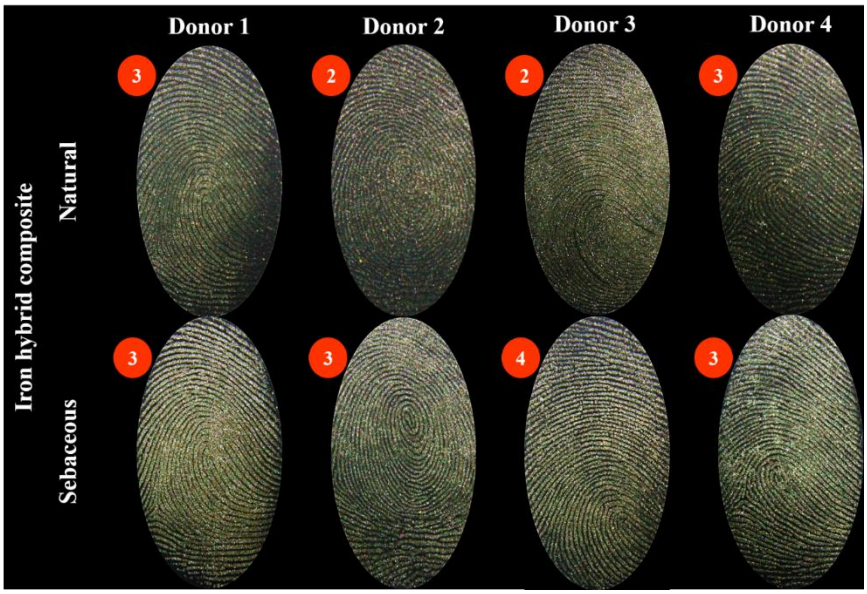

Figure 6. Natural and sebaceous fingerprints developed with the Fe hybrid composite and their respective scores.

Figures 7 and 8 represent a depletion series from donor 3, developed with copper and iron composites. In Supplementary Figures S2–S7, the depletion series from the other donors developed with both composites can be observed.

Preprints.org (www.preprints.org) | NOT PEER-REVIEWED | Posted: 10 October 2024 doi:10.20944/preprints202410.0766.v1

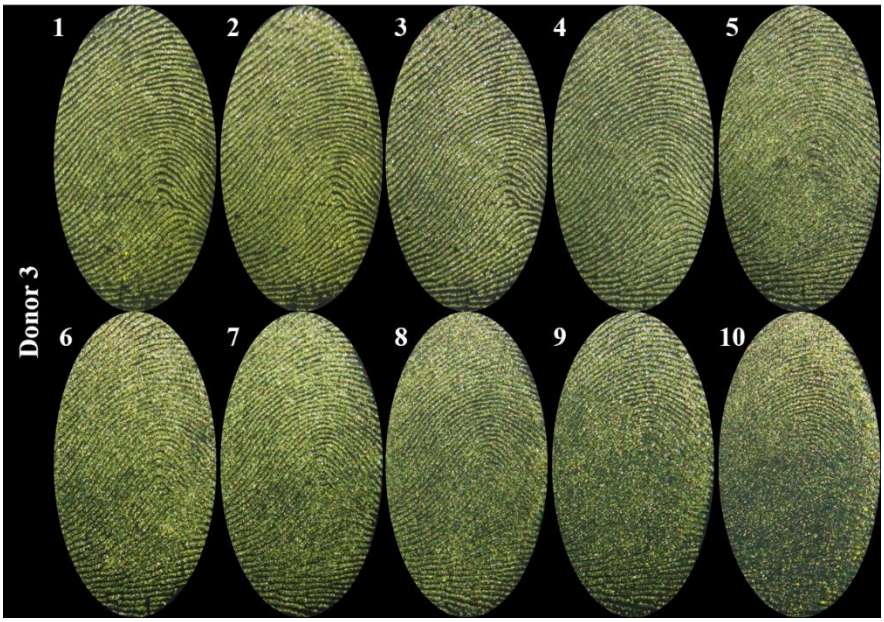

Figure 7. Depletion series developed with the Cu composite from donor 3.

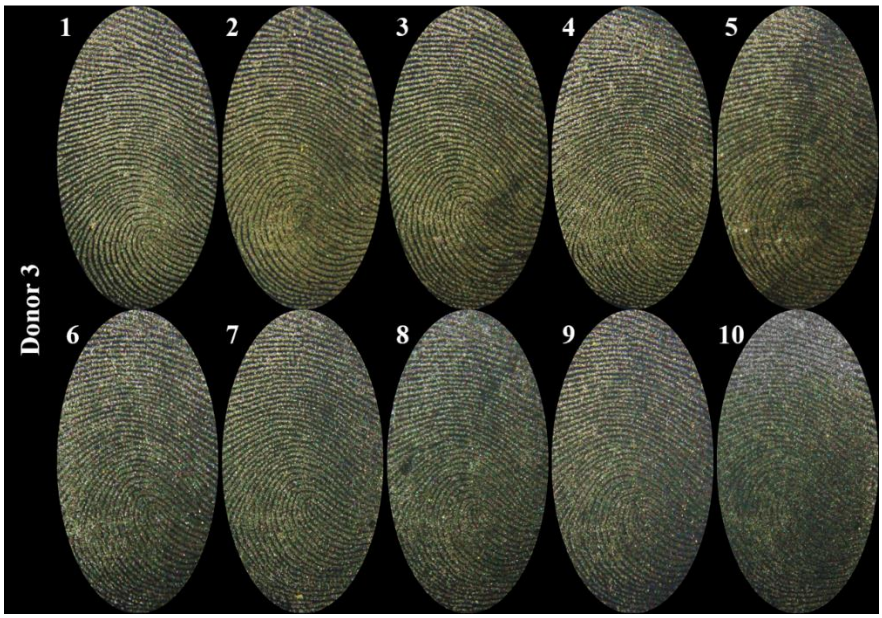

Figure 8. Depletion series developed with the Fe composite from donor 3.

Figure 9 shows the same fingerprint (natural and sebaceous) developed on the left with composites and on the right with commercial gold powder. Supplementary Figures S8 and S9 display the development achieved for the same natural and sebaceous fingerprints from the other donors, using both composites and the commercial powder.

Preprints.org (www.preprints.org) | NOT PEER-REVIEWED | Posted: 10 October 2024 doi:10.20944/preprints202410.0766.v1

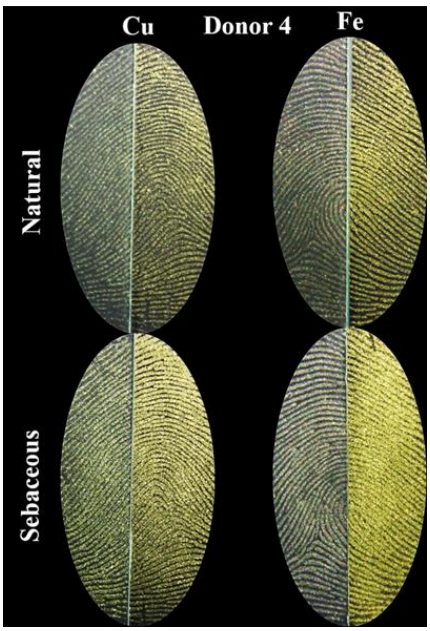

Figure 9. Half-and-half fingerprint (Natural (N) and sebaceous (S)) from donor 4, with the left half developed using composites and the right half with Gold® commercial powder purchased from Sirchie®.

The SEM images (Figure 10) provided a detailed analysis of the development of latent fingerprints using both composites. Magnifications of 40x, 600x, and 2000x were applied to investigate the minutiae of the fingerprints, the interaction of the particles with the surface, and the shape and size of the particles. For this analysis, latent fingerprints, both natural and sebaceous, were deposited on glass surfaces and developed with Cu and Fe composites. These magnification levels offered a more precise view of the particle adhesion to the ridges of the fingerprints and the effectiveness of the composites in developing the fingerprints.

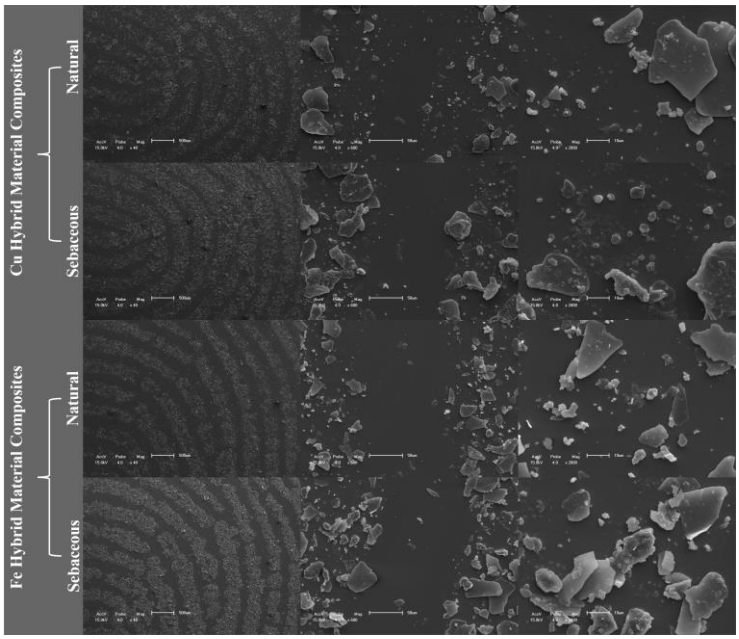

Figure 10. SEM analysis of natural and sebaceous latent fingerprints developed with Cu and Fe composites on a glass surface.

4. Discussion

Preprints.org (www.preprints.org) | NOT PEER-REVIEWED | Posted: 10 October 2024 doi:10.20944/preprints202410.0766.v1

According to the literature, it is known that the conjugated β-diketone portion of curcumin is a strong chelating agent, being capable of interacting with several metal ions through a coordination bond, which can modify the color of the organic phase of curcumin [46,47]. Thus, the colorimetry results indicated the effective formation of hybrid materials, evidenced by the color change after the addition of these metals and confirmed by their concentration found in the materials.

Thus, UV-Vis, X-ray and FT-IR results suggests that the one-pot synthesis was efficient in forming hybrid materials using *Kappa*-carrageenan as a reducing agent. A strong absorption in the 400-550 nm range of UV-Vis spectrum (Figure 2A) was observed for all samples, corresponding to the blue and green light region, which agrees with the colorimetric results. The shift in wavelength from curcumin to the hybrid materials suggests an interaction between the carbonyl group of curcumin in metal coordination [39]. XRD analysis (Figure 2B) of curcumin confirmed its typical crystalline structure [40], while both *Kappa*-carrageenan and the hybrid materials exhibited amorphous structures. FT-IR was used to identity the functional groups on the surface of the samples and the results are displayed in Figures 2C and 2D. The infrared spectra of curcumin show a characteristic band at 3461 cm-1 corresponding to the phenolic stretching (O-H). The aromatic stretching of (C=C) and stretching vibrations of (C=C) were observed at 1629 cm-1 and 1509 cm-1, respectively. The stretching vibrations of (C=O) were observed at 1599 cm-1, while the bending vibrations corresponding (C-H) and aromatic stretching of (C-O) vibrations were noticed at 1427 cm-1 and 1280 cm-1, respectively. Finally, stretching vibrations related to (C-O-C) were observed at 1025 cm-1 [42]. The FT-IR of the Fe and Cu hybrid materials shown in Figure 2-C and D, exhibited similar bands as observed in the curcumin, with shifts in wavenumber indicating changes in the vibrational state of curcumin upon binding to the metal ions [43,44].

The thermal stability of hybrid materials is crucial for their practical applications. *Kappa*-carrageenan exhibited three thermal events (Figure 3A): the first corresponding to moisture loss, while the second and third events were related to the decomposition of the carbohydrate skeleton and complete degradation. Curcumin began with the dehydroxylation process, followed by its total degradation. The Curcumin/*Kappa*-carrageenan composite showed similar behavior to pure *Kappa*-carrageenan (Figure 3B). On the other hand, the hybrid materials, displayed differences due to the varying amounts of curcumin present in the samples. Thus, the TGA curves indicate that the hybrid materials possess superior thermal stability than pure curcumin [34].

The presence of three peaks in the chromatogram (Figure S1 – Supplementary information) can be explained by the composition of commercial curcumin (65%), which contains two other curcuminoids: desmethoxycurcumin and bisdemethoxycurcumin [48], representing the remaining 35% of the sample. Thus, the method adapted proved to be efficient, as the three peaks did not overlap. In addition, it provided a fast analysis time of 5 minutes [33]. The curcuminoid diferuloylmethane, commonly known as curcumin, is the largest fraction present in the sample, as curcumin was acquired at 65% purity. Therefore, the peak referring to the retention time of 3.263 minutes, which has the greatest area and intensity, represents curcumin. Desmethoxycurcumin is the second largest fraction of the sample and was identified with a retention time of 3.103 minutes. Finally, bisdemethoxycurcumin, which denotes the smallest fraction of the sample, was identified with a retention time of 2.957 minutes. Several reports described the same order of curcuminoids with bisdemethoxycurcumin being the first peak and curcumin the last peak [49,50], the impurities in curcumin sample, no interference in the formation of hybrid materials were found, since all curcuminoids contain the β-diketone fraction responsible for binding the metals. The absence or presence of methoxy groups (the only difference between the curcuminoids) does not influence the process, as they remain intact after the synthesis of the hybrid materials [18].

Regarding curcumin degradation, studies using curcumin dissolved in ethanol [42] or in Phosphate Buffered Saline (PBS) buffer [16] reported vanillin, vanillic acid, and ferulic acid as degradation products [18,51]. In this study, samples were dissolved in acetonitrile, resulting in degradation after 24 h, as observed by multiple peaks in the chromatogram of Figure 5B, indicating the formation of other molecules, i.e., degradation products. Additionally, a decrease in the curcumin peak intensity from 450 at time zero to 55 after 24 hours, along with a considerable reduction in peak

Preprints.org (www.preprints.org) | NOT PEER-REVIEWED | Posted: 10 October 2024 doi:10.20944/preprints202410.0766.v1

area, confirmed the generation of degradation products. However, the same behavior was not observed in the chromatograms of the copper hybrid materials (Figure 4C) and the iron hybrid materials (Figure 4D), suggesting that the hybrid materials offer superior stability compared to isolated curcumin.

The use of powders to develop fingerprints, it is crucial to address the limitations of curcumin, especially in terms of stability. The previous results demonstrated that the combination of curcumin with Cu and Fe metals has led to a significant increase in stability of the samples, which is one of the key requirements for practical use [52,53]. Based on these results, the potential of these compounds as developers for latent fingerprints was investigated. Composites were applied to fingerprints from various donors, aiming to capture variations related to age, sex, and other characteristics. It is known that factors such as occupation, health (both physical and mental), diet, and medications directly affect the fingerprint composition, both natural and sebaceous fingerprints were evaluated to assess interactions with the water-soluble and lipid-soluble compounds [24,54]. Through the method of Sears et al., (2012) [37], the visual appearance of the fingerprints was converted to numerical values for classification. The results demonstrated that both composites were effective in developing natural and sebaceous fingerprints from all donors, resulting in clear images on glass surfaces. The composites adhered to the fingerprints without having adhesion to the glass, providing good contrast in the images (Figures 5 and 6). In numerical values, the lowest scores, such as zero (no evidence of mark) and one (evidence of contact without ridge details), were not assigned to any fingerprint developed with the composites. Only one natural fingerprint of the Cu hybrid composite and two from the Fe hybrid composite received a score of 2, indicating limited development (with about 1/3 of ridge details present, but insufficient for identification). The remaining fingerprints were rated with scores of 3 or 4, reflecting identifiable and well-developed marks. The Cu composite (Figure 5) showed better performance in developing sebaceous fingerprints, receiving a score of 4 for donors 2, 3, and 4. For natural fingerprints, donor 1 received a score of 4, while donors 3 and 4 received a score of 3. Similarly, the Fe composite (Figure 6) also demonstrated superior performance in sebaceous fingerprints compared to natural ones. Donors 1 and 4 had natural fingerprints rated 3, while all sebaceous fingerprints were rated 3, except for donor 3, who received a score of 4, indicating identifiable and detailed fingerprints for all donors. These findings indicate that, although the same deposition and development method was applied consistently, the influence of the donor on the development process was evident. Nevertheless, the results were consistent and satisfactory, with the Cu composite showing higher contrast and better scores compared to the Fe composite.

To evaluate the sensitivity of the composites in developing fingerprints, depletion series were performed. These series consist of successive contacts of the same finger with the surface, resulting in a progressive reduction in the amount of residue left with each new contact. Thus, the effective development of fingerprints left in the final contact indicate higher sensitivity of the developing powder, as there is less material available for adhesion [37]. Figures 7 and 8 present the depletion series for donor 3, developed with Cu and Fe composites, respectively. Although the Cu composite showed better performance in the previously discussed fingerprints, when comparing the depletion series for donor 3, greater clarity was observed in the revelations made with the Fe composite. This composite demonstrated good development, with excellent sharpness and contrast in most deposits, except for the tenth, where there was a significant decrease in quality. On the other hand, the Cu composite showed better clarity in the first four deposits, but from the fifth onward, there was a progressive decline in the quality of development. This decline may be attributed to the higher contrast provided by the Cu composite, which could have hindered the clarity of the fingerprints in deposits with less sebaceous residue. Similar results were observed for the other donors in the depletion series, as shown in Supplementary Figures 2 to 7. Although the Fe composite offers lower contrast compared to Cu, it demonstrated superior sharpness in the depletion series for all donors, often effectively revealing fingerprints up to the tenth deposit. In contrast, the Cu composite showed satisfactory development with good up to the fourth deposit, followed by a progressive decline in quality from the fifth onward.

Preprints.org (www.preprints.org) | NOT PEER-REVIEWED | Posted: 10 October 2024 doi:10.20944/preprints202410.0766.v1

It is important to consider that fingerprints exhibit inherent variability in their composition, including factors such as chemical composition, the amount of material deposited, and the pressure applied during deposition. To minimize the impact of these variables on fingerprint development, the use of half-and-half fingerprint tests is an effective approach. In this method, fingerprints are deposited and physically split along the centerline, allowing each half to be developed using different techniques or powders (powdering method) [37]. This "half-and-half" strategy, applied to the comparative analysis between synthesized powders and commercially available powders, is particularly relevant as it allows the evaluation of whether the developed material performs similarly to those currently used by the Federal Police [32]. Figure 9 illustrates the natural and sebaceous fingerprints of donor 4, developed using the half-and-half method. The left halves were developed with Cu or Fe composites, while the right halves were developed with the commercial gold powder. A good development of natural fingerprints was observed with both composites, exhibiting quality comparable to that of the commercial gold powder. In the case of sebaceous fingerprints, the Cu composite showed performance similar to that of the commercial powder, while the Fe composite demonstrated superior sharpness compared to the commercial powder. Figures S8 and S9 (Supplementary information) show the half-and-half fingerprints of the other donors. A similar behavior was observed in the development of the composites, with performance equivalent to or better than the commercial powder. When comparing both composites, the Fe one stood out by providing greater sharpness, resulting in clearer definition of fingerprint minutiae.

So far, hybrid material composites have been evaluated as developers for latent fingerprints using various methods, all applied to glass surfaces. Considering that the surface on which a fingerprint is deposited can significantly influence the effectiveness of its development, the final analysis of these powders included tests on surfaces representative of those encountered in operational work. For this, the same composites were applied to different surfaces commonly found in forensic investigations [37]. Examples of these surfaces can be seen in Figure 11.

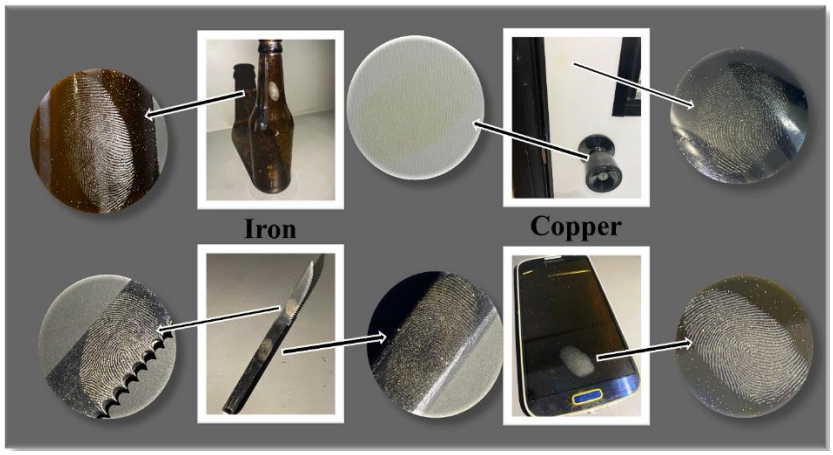

Figure 11. Development of latent fingerprints using Cu and Fe composites on different objects representing porous and non-porous surfaces: glass bottle, doorknob and door, knife and knife handle, and a black smartphone.

Figure 11 illustrates the development of latent fingerprints with both composites on porous and non-porous surfaces. Objects commonly found in real-world scenarios were selected, including glass bottles, metal knife surfaces, plastic knife handles, wooden door surfaces, metal doorknobs, and the glass screens of smartphones. Both composites were effective in enhancing latent fingerprints on both light and dark surfaces, as well as porous and non-porous ones, demonstrating the versatility of the developed powders. The revealed fingerprints exhibited sufficient detail to be used in human identification processes.

The SEM images (Figure 10) provided a detailed analysis of the minutiae in both natural and sebaceous fingerprints developed with both Fe and Cu composites. At 40x magnification, it was observed that the Fe composite offered greater clarity compared to the Cu composite, which is

Preprints.org (www.preprints.org) | NOT PEER-REVIEWED | Posted: 10 October 2024 doi:10.20944/preprints202410.0766.v1

directly related to the strong adhesion of the Fe composite to the fingerprint compounds, while interacting minimally with the glass surface, as evidenced in the 600x magnified images. Regarding morphology, both composites exhibited irregular shapes and heterogeneous particle size [28], ranging from 50 micrometers to less than 10 micrometers. Despite these characteristics, the composites were effective in developing latent fingerprints, providing sufficient detail for human identification.

5. Conclusions

The hybrid copper and iron materials were synthesized via one-pot methodology using natural curcumin and *Kappa*-carrageenan as a reducing agent. These materials were characterized by different techniques such as FT-IR, UV-Vis, XRD and F AAS. The observed color changes and enhanced stability of these materials can be attributed to the coordination of Cu^{2+} or Fe^{3+} metal ions with curcumin, as well as potential interactions with *Kappa*-carrageenan. To verify whether curcumin hybridization effectively improved its stability, thermogravimetric analysis was performed, showing that the hybrid materials had greater thermal stability than curcumin. Solution stability studies using liquid chromatography revealed that curcumin showed degradation product peaks after 24 hours of solvent exposure, whereas the hybrid materials remained stable after 24 hours. The hybrid composites were further applied as latent fingerprint developers. The results showed that both materials effectively developed natural and sebaceous fingerprints from various donors, with good clarity and contrast on glass surfaces. In successive contact depletion series, the Fe composite demonstrated higher sensitivity, revealing sharpness fingerprints up to the tenth contact, while the Cu composite showed less quality after the fifth contact. In comparative tests with commercial gold powder, both hybrid materials performed similarly, with the Fe composite standing out for its fingerprint sharpness. Additionally, when applied to surfaces representative of forensic scenarios (such as glass bottles, metal doorknobs, knife surfaces, and smartphones), the composites were versatile, revealing sufficient fingerprint details for human identification on both porous and non-porous surfaces. Overall, these findings highlight the potential of hybrid materials to enhance forensic applications and contribute to the sustainable use of natural resources.

Supplementary Materials: The following supporting information can be downloaded at the website of this paper posted on Preprints.org, Table S1: Classification scheme used for the evaluation of developed fingerprint; Table S2: Color parameters of reagents and hybrids materials; Figure S1: Chromatogram of commercial natural curcumin; Figure S2: Depletion series developed with the Cu composite from donor 1; Figure S3: Depletion series developed with the Fe composite from donor 1; Figure S4: Depletion series developed with the Cu composite from donor 2; Figure S5: Depletion series developed with the Fe composite from donor 2; Figure S6: Depletion series developed with the Cu composite from donor 4; Figure S7: Depletion series developed with the Fe composite from donor 4; Figure S8: Half-and-half fingerprint (Natural (N) and sebaceous (S)) from donors 1, 2 and 3, with the left half developed using Cu composite and the right half with Gold® commercial powder purchased from Sirchie; Figure S9: Half-and-half fingerprint (Natural (N) and sebaceous (S)) from donors 1, 2 and 3, with the left half developed using Fe composite and the right half with Gold® commercial powder purchased from Sirchie®.

Author Contributions: Conceptualization, D.T.P.; methodology, D.T.P.; validation, A.F.L; formal analysis, D.H.B., B.V.L., D.A.G. and M.P.G.; investigation, D.T.P., A.F.L., J.P.S. and G.Q.J.; data curation, T. P. and B. N. R.; writing—original draft preparation, D.T.P.; writing—review and editing, A.F.L. and G.K.M.; supervision, C.M.P.P., A.L.M. and N.L.V.C.; funding acquisition, C.M.P.P.; project administration, C.M.P.P. All authors have read and agreed to the published version of the manuscript.

Funding: Financial support for this research by FAPERGS (Research Support Foundation of the Rio Grande do Sul State 22/2551-0000840-2), Coordination for Improvement of Higher-Level Personnel (CAPES), and the Forensic National Institute of Science and Technology Grant number (465450/2014-8).

Informed Consent Statement: Not applicable.

Data Availability Statement: The data can be made available on request.

Acknowledgments: The authors are thankful to FAPERGS, CAPES, Forensic National Institute of Science and Technology, and the Brazilian Federal Police for their assistance.

Preprints.org (www.preprints.org) | NOT PEER-REVIEWED | Posted: 10 October 2024 doi:10.20944/preprints202410.0766.v1

Conflicts of Interest: The authors declare no conflicts of interest.

References

1. Barros, H. L.; Tavares, L.; Stefani, V. Dye-doped starch microparticles as a novel fluorescent agent for the visualization of latent fingermarks on porous and non-porous substrates. *Forensic Chemistry*, **2020**, 20, 100264.
2. Khare, V.; Singla, A. A review on the advancements in chemical examination of composition of latent fingerprint residues. *Egyptian Journal of Forensic Sciences*, **2022**, 12, 1.
3. Robson, R.; Ginige, T.; Mansour, S.; Khan, I.; Assi, S. Analysis of fingermark constituents: A systematic review of quantitative studies. *Chemical Papers*, **2022**, 76, 8, 4645-4667.
4. Li, L.; Li, Q.; Chu, J.; Xi, P.; Wang, C.; Liu, R.; Wang, X.; Cheng, B. Dual-mode luminescent multilayer core-shell UCNPs@ SiO2@ TEuTbB nanospheres for high-level anti-counterfeiting and recognition of latent fingerprints. *Applied Surface Science*, **2022**, 581, 152395.
5. Ansari, A. A.; Aldajani, K. M.; AlHazaa, A. N.; Albrithen, H. A. Recent progress of fluorescent materials for fingermarks detection in forensic science and anti-counterfeiting. *Coordination Chemistry Reviews*, **2022**, 462, 214523.
6. Poletti, T. Avalição química e aplicação de curcuminas derivadas de cinamaldeído como potenciais reveladores de impressões digitais. Dissertation, Master's degree, Federal University of Pelotas, Pelotas – Brazil, 2021.
7. Passos, L. F.; Berneira, L. M.; Poletti, T.; Mariotti, K. D. C.; Carreño, N. L.; Hartwig, C. A.; Pereira, C. M. Evaluation and characterization of algal biomass applied to the development of fingermarks on glass surfaces. *Australian Journal of Forensic Sciences*, **2021**, 53, 3, 337-346.
8. Pereira, C. M.; Pacheco, B. S.; da Silva, C. C. *Curcumin and analogues: chemical and biological aspects*, 2017, LAP LAMBERT Academic Publishing.
9. Arab, C.; El Kurdi, R.; Patra, D. Effect of pH on the removal of anionic and cationic dyes using zinc curcumin oxide nanoparticles as adsorbent. *Materials Chemistry and Physics*, **2022**, 277, 125504.
10. Verma, R. K.; Kumari, P.; Maurya, R. K.; Kumar, V.; Verma, R. B.; Singh, R. K. Medicinal properties of turmeric (Curcuma longa L.): A review. *International Journal of Chemical Studies*, **2018**, 6, 4, 1354–1357.
11. Yang, M. Y.; Chang, K. C.; Chen, L. Y.; Hu, A. Low-dose blue light irradiation enhances the antimicrobial activities of curcumin against Propionibacterium acnes. *Journal of Photochemistry and Photobiology B: Biology*, **2018**, 189, 21-28.
12. Maghsoudi, A.; Yazdian, F.; Shahmoradi, S.; Ghaderi, L.; Hemati, M.; Amoabediny, G. Curcumin-loaded polysaccharide nanoparticles: Optimization and anticariogenic activity against Streptococcus mutans. *Materials Science and Engineering*, **2017**, 75, 1259-1267.
13. Lin, L.; Li, C.; Zhang, D.; Yuan, M.; Chen, C. H.; Li, M. Synergic effects of berberine and curcumin on improving cognitive function in an Alzheimer's disease mouse model. *Neurochemical research*, **2020**, 45(5), 1130-1141.
14. Buliga, D. I.; Diacon, A.; Calinescu, I.; Popa, I.; Rusen, E.; Ghebaur, A.; Tutunaru, O.; Boscornea, C. A. Enhancing the light fastness of natural dyes by encapsulation in silica matrix. *Journal of Photochemistry and Photobiology A: Chemistry*, **2022**, 432, 114085.
15. Souza, C. R. A.; Osme, S. F.; Glória, M. B. A. Stability of curcuminoid pigments in model systems. *Journal of Food Processing and Preservation*, **1997**, 21, 5, 353–363.
16. Kumar, P.; Saha, T.; Behera, S.; Gupta, S.; Das, S.; Mukhopadhyay, K. Enhanced efficacy of a Cu2+ complex of curcumin against Gram-positive and Gram-negative bacteria: Attributes of complex formation. *Journal of Inorganic Biochemistry*, **2021**, 222, 111494.
17. Hernández, M.; Felipe, C.; Guzmán-Vargas, A.; Rivera, J. L.; Lima, E. Highly Stable Hybrid Pigments Prepared from Organic Chromophores and Fluorinated Hydrotalcites. *Colorants*, **2024**, 3, 2, 125-135.
18. Prasad, S.; Lall, R. Zinc-Curcumin Based Complexes in Health and Diseases: An Approach in Chemopreventive and Therapeutic Improvement. *Journal of Trace Elements in Medicine and Biology*, **2022**, 73, 127023.
19. Silvério, F. Preparação e Caracterização de Materiais Híbridos Formados Pela Interação Entre Hidróxidos Duplos Lamelares e Siliconas Aniônicas. Thesis, Doctorate's degree, Federal University of São Paulo, São Paulo – Brazil, 2009.
20. Lee, J. Y.; Lee, S.; Choi, J. H.; Na, K. ι-Carrageenan nanocomposites for enhanced stability and oral bioavailability of curcumin. *Biomaterials research*, **2021**, 25, 1, 32.
21. Tan, K. X.; Ng, L. L. E.; Loo, S. C. J. Formulation development of a food-graded curcumin-loaded medium chain triglycerides-encapsulated *kappa* carrageenan (Cur-mct-kc) gel bead based oral delivery formulation. *Materials*, **2021**, 14, 11.
22. Wan, H.; Li, C.; Mahmud, S.; Liu, H. *Kappa* carrageenan reduced-stabilized colloidal silver nanoparticles for the degradation of toxic azo compounds. *Colloids and Surfaces A: Physicochemical and Engineering Aspects*, **2021**, 616, 126325.

Preprints.org (www.preprints.org) | NOT PEER-REVIEWED | Posted: 10 October 2024 doi:10.20944/preprints202410.0766.v1

23. Leitzke, A. F.; Berneira, L. M.; Rosa, B. N. D.; Moreira, B. C.; Mariotti, K. D. C.; Venzke, D.; Pereira, C. M. A Química de Produtos Naturais aplicados a reveladores de impressões digitais latentes. *Química Nova*, **2022**, 45, 424-434.
24. Bueno, D. T.; Leitzke, A. F.; Crizel, R. L.; Jansen-Alves, C.; Bertizzolo, E. G.; da Silva, J. P.; Sejanes, G. Q.; Mariotti, K. C.; de Pereira, C. M. P. Characterization of Bixin by UV-Visible Spectroscopy and HPLC, and Its Application as Latent Fingermark Developer. *Analytica*, **2024**, 5, 1, 107-118.
25. Balsan, J. D.; Rosa, B. N.; Pereira, C. M.; Santos, C. M. Desenvolvimento de metodologia de revelação de impressão digital latente com chalconas. *Química Nova*, **2019**, 42, 8, 845-850.
26. da Rosa, B. N.; da Rosa, M. P.; Poletti, T.; de Lima, N. P. K.; Maron, G. K.; Lopes, B. V.; Mariotti, K. C.; Beck, P. H.; Carreno, N. L. V.; de Pereira, C. M. P. Green composites from thiophene chalcones and rice husk lignin: an alternative of powder for latent fingermark. *Surfaces*, **2022**, 5, 4, 481-488.
27. da Rosa, B. N.; Maron, G. K.; Lopes, B. V.; Rocha, A. C. S.; de Moura Gatti, F.; Machado, J. O. A.; Barichello, J. M.; Mariotti, K. C.; Trossini, G. H. G.; Carreno, N. L. V.; Pereira, C. M. P. Dimethylaminochalcones with silicon dioxide and zinc oxide as latent fingermark developer powder. *Materials Chemistry and Physics*, **2023**, 295, 127033.
28. Pacheco, B. S.; Da Silva, C. C.; Da Rosa, B. N.; Mariotti, K. C.; Nicolodi, C.; Poletti, T.; Segatto, N. V.; Collares, T.; Seixas, F. K.; Paniz, O.; Carreño, N. L. V.; Pereira, C. M. Monofunctional curcumin analogues: evaluation of green and safe developers of latent fingerprints. *Chemical Papers*, **2021**, 75, 3119-3129.
29. Poletti, T.; Berneira, L. M.; Passos, L. F.; da Rosa, B. N.; de Pereira, C. M.; Mariotti, K. D. C. Preliminary efficiency evaluation of development methods applied to aged sebaceous latent fingermarks. *Science & Justice*, **2021**, 61, 4, 378-383.
30. Venzke, D.; Poletti, T.; Rosa, B. N.; Berneira, L. M.; de Lima, N. P.; de Oliveira, T. F.; Carreno, N. L. V.; Mariotti, K. C.; Duarte, L. S.; Nobre, S. M.; Pereira, C. M. Preparation of fluorescent bisamides: a new class of fingermarks developers. *Chemical Data Collections*, **2021**, 33, 100680.
31. Lima, N. P.; Rosa, B. N.; Poletti, T.; Moreira, B. C.; Leitzke, A. F.; Mariotti, K. C., Carreno, N. L. V.; Pereira, C. M. As clássicas hidrazonas como reveladores de impressões digitais: uma proposta de química orgânica experimental. *Química Nova*, **2023**, 46, 02, 215-221.
32. Leitzke, A. F.; Bueno, D. T.; Poletti, T.; Maron, G. K.; Lopes, B. V.; Morais, E. V.; Inacio, A. P. O. L.; Silveira, C. I.; Silva, J. P.; Dias, D.; Carreño, N. L. V.; Pereira, C. M. P. D. The effectiveness of natural indigo/kaolinite composite powder in the development of latent fingermarks. *Egyptian Journal of Forensic Sciences*, **2024**, 14, 1, 19.
33. Li, S.; Mu, B.; Yan, P.; Kang, Y.; Wang, Q.; Wang, A. Incorporation of different metal ion for tuning color and enhancing antioxidant activity of curcumin/palygorskite hybrid materials. *Frontiers in Chemistry*, **2021**, 9, 760941.
34. Anjani, Q. K.; Utomo, E.; Domínguez-Robles, J.; Detamornrat, U.; Donnelly, R. F.; Larrañeta, E. A new and sensitive HPLC-UV method for rapid and simultaneous quantification of curcumin and D-panthenol: application to in vitro release studies of wound dressings. *Molecules*, **2022**, 27, 6, 1759.
35. Modwi, A.; Ali, M. K. M.; Taha, K. K.; Ibrahem, M. A.; El-Khair, H. M.; Eisa, M. H.; Elamin, M. R.; Aldaghri, O.; Alhathlool, R.; Ibnaouf, K. H. Structural and optical characteristic of chalcone doped ZnO nanoparticles. *Journal of Materials Science: Materials in Electronics*, **2018**, 29, 2791-2796.
36. Fioravanti, M. I. A.; Pizano, F, P.; Rebellato, A. P.; Milani, R. F.; Morgano, M. A.; Bragotto, A. P. A. Turmeric products: Evaluation of curcumin and trace elements. *Food Research International*, **2024**, 196, 115028.
37. Sears, V. G.; Bleay, S. M.; Bandey, H. L.; Bowman, V. J. A methodology for finger mark research. *Science & Justice*, **2012**, 52, 3, 145-160.
38. Subhan, M. A.; Alam, K.; Rahaman, M. S.; Rahman, M. A.; Awal, R. Synthesis and characterization of metal complexes containing curcumin (C21H20O6) and study of their anti-microbial activities and DNA binding properties. *J. Sci. Res*, **2014**, 6, 1, 97-109.
39. Zhou, S. S.; Xue, X.; Wang, J. F.; Dong, Y.; Jiang, B.; Wei, D.; Wan, M.; Jia, Y. Synthesis, optical properties and biological imaging of the rare earth complexes with curcumin and pyridine. *Journal of Materials Chemistry*, **2012**, 22, 42, 22774-22780.
40. Sayyar, Z.; Malmiri, H. J. Photocatalytic and antibacterial activities study of prepared self-cleaning nanostructure surfaces using synthesized and coated ZnO nanoparticles with Curcumin nanodispersion. *Zeitschrift fur Kristallographie - Crystalline Materials*, **2019**, 234, 5, 307–328.
41. Kanmani, P.; Rhim, J. W. Development and characterization of carrageenan/grapefruit seed extract composite films for active packaging. *International Journal of Biological Macromolecules*, **2014**, 68, 258–266.
42. Chen, X.; Zou, L. Q.; Niu, J.; Liu, W.; Peng, S. F.; Liu, C. M. The stability, sustained release and cellular antioxidant activity of curcumin nanoliposomes. *Molecules*, **2015**, 20, 8, 14293-14311.
43. Halevas, E.; Papadopoulos, T. A.; Swanson, C. H.; Smith, G. C.; Hatzidimitriou, A.; Katsipis, G.; Katsipis, G.; Pantazaki, A.; Sanakis, I.; Ypsilantis, K.; Litsardakis, G.; Salifoglou, A. In-depth synthetic, physicochemical and in vitro biological investigation of a new ternary V (IV) antioxidant material based on curcumin. *Journal of Inorganic Biochemistry*, **2019**, 191, 94-111.

Preprints.org (www.preprints.org) | NOT PEER-REVIEWED | Posted: 10 October 2024 doi:10.20944/preprints202410.0766.v1

44. Halevas, E.; Pekou, A.; Papi, R.; Mavroidi, B.; Hatzidimitriou, A. G.; Zahariou, G.; Litsardakis, G.; Sagnou, M.; Pelecanou, M.; Pantazaki, A. A. Synthesis, physicochemical characterization and biological properties of two novel Cu (II) complexes based on natural products curcumin and quercetin. *Journal of inorganic biochemistry*, **2020**, 208, 111083.
45. Kulal, P.; Badalamoole, V. Hybrid nanocomposite of *kappa*-carrageenan and magnetite as adsorbent material for water purification. *International Journal of Biological Macromolecules*, **2020**, 165, 542–553.
46. de França, B. M.; Oliveira, S. S.; Souza, L. O.; Mello, T. P.; Santos, A. L.; Forero, J. S. B. Synthesis and photophysical properties of metal complexes of curcumin dyes: Solvatochromism, acidochromism, and photoactivity. *Dyes and Pigments*, **2022**, 198, 110011.
47. Prasad, S.; DuBourdieu, D.; Srivastava, A.; Kumar, P.; Lall, R. Metal–curcumin complexes in therapeutics: an approach to enhance pharmacological effects of curcumin. *International journal of molecular sciences*, **2021**, 22, 13, 7094.
48. Sharifi-Rad, J.; Rayess, Y. E.; Rizk, A. A.; Sadaka, C.; Zgheib, R.; Zam, W.; Sestito, S.; Rapposelli, S.; Neffe-Skocinska, K.; Zielinska, D.; Salehi, B.; Setzer, W. N.; Dosoky, N. S.; Taheri, Y.; Beyrouthy, M. E.; Martorell, M.; Ostrander, E. A.; Suleria, H. A. R.; Cho, W. C.; Maroyi, A.; Martins, N. Turmeric and its major compound curcumin on health: bioactive effects and safety profiles for food, pharmaceutical, biotechnological and medicinal applications. *Frontiers in pharmacology*, **2020**, 11, 550909.
49. Bonifácio, D.; Martins, C.; David, B.; Lemos, C.; Neves, M. G. P. M. S.; Almeida, A.; Pinto, D. C. G. A.; Cunha, Â. Photodynamic inactivation of Listeria innocua biofilms with food-grade photosensitizers: a curcumin-rich extract of Curcuma longa vs commercial curcumin. *Journal of applied microbiology*, **2018**, 125, 1, 282-294.
50. Chen, Y. C.; Chen, B. H. Preparation of curcuminoid microemulsions from: Curcuma longa L. to enhance inhibition effects on growth of colon cancer cells HT-29. *RSC Advances*, **2018**, 8, 5, 2323–2337.
51. Khurana, Amrik; Ho, C.-T. High Performance Liquid Chromatographic Analysis of Curcuminoids and Their Photo-Oxidative Decomposition Compounds in Curcuma Longal. *Journal of Liquid Chromatography*, **1988**, 11, 11, 2295–2304.
52. Chávez, D.; Garcia, C. R.; Oliva, J.; Diaz-Torres, L. A. A review of phosphorescent and fluorescent phosphors for fingerprint detection. *Ceramics International*, **2021**, 47, 1, 10-41.
53. Vadivel, R.; Nirmala, M.; Anbukumaran, K. Commonly available, everyday materials as non-conventional powders for the visualization of latent fingerprints. *Forensic Chemistry*, **2021**, 24, 100339.
54. De Alcaraz-Fossoul, J.; Mestres Patris, C.; Balaciart Muntaner, A.; Barrot Feixat, C.; Gené Badia, M. Determination of latent fingerprint degradation patterns—a real fieldwork study. *International Journal of Legal Medicine*, **2013**, 127, 857-870.

Disclaimer/Publisher's Note: The statements, opinions and data contained in all publications are solely those of the individual author(s) and contributor(s) and not of MDPI and/or the editor(s). MDPI and/or the editor(s) disclaim responsibility for any injury to people or property resulting from any ideas, methods, instructions or products referred to in the content.